Membrane Biology:

Conformational Changes Produced by ATP Binding to the Plasma Membrane Calcium Pump

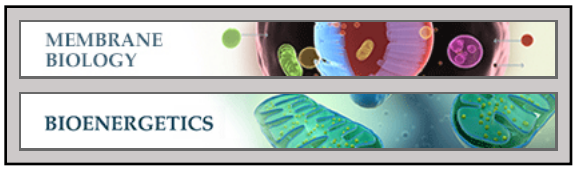

Irene C. Mangialavori, Mariela S. Ferreira-Gomes, Nicolás A. Saffioti, Rodolfo M. González-Lebrero, Rolando C. Rossi and Juan Pablo F. C. Rossi

J. Biol. Chem. 2013, 288:31030-31041.
doi: 10.1074/jbc.M113.494633 originally published online September 11, 2013

THE JOURNAL OF BIOLOGICAL CHEMISTRY VOL. 288, NO. 43, pp. 31030–31041, October 25, 2013

Conformational Changes Produced by ATP Binding to the Plasma Membrane Calcium Pump*

Received for publication, June 17, 2013, and in revised form, August 21, 2013 Published, JBC Papers in Press, September 11, 2013, DOI 10.1074/jbc.M113.494633

Irene C. Mangialavori[1], Mariela S. Ferreira-Gomes[1], Nicolás A. Saffioti, Rodolfo M. González-Lebrero, Rolando C. Rossi[2], and Juan Pablo F. C. Rossi[3]

From the Instituto de Química y Fisicoquímica Biologicas, Facultad de Farmacia y Bioquímica, Universidad de Buenos Aires, Consejo Nacional de Investigaciones Científicas y Técnicas, Junín 956 (1113) Buenos Aires, Argentina

Background: The plasma membrane calcium ATPase (PMCA) reaction cycle is associated with conformational changes.
Results: We identified different conformations after the association of Ca^{2+}, ATP, and vanadate to PMCA.
Conclusion: PMCA forms a stable complex with Ca^{2+} and vanadate; ATP can bind to all pump conformations.
Significance: This study found a new intermediate in the PMCA reaction cycle; all of the intermediates interact with ATP.

The aim of this work was to study the plasma membrane calcium pump (PMCA) reaction cycle by characterizing conformational changes associated with calcium, ATP, and vanadate binding to purified PMCA. This was accomplished by studying the exposure of PMCA to surrounding phospholipids by measuring the incorporation of the photoactivatable phosphatidylcholine analog 1-*O*-hexadecanoyl-2-*O*-[9-[[[2-[^{125}I]iodo-4-(trifluoromethyl-3H-diazirin-3-yl)benzyl]oxy]carbonyl]nonanoyl]-*sn*-glycero-3-phosphocholine to the protein. ATP could bind to the different vanadate-bound states of the enzyme either in the presence or in the absence of Ca^{2+} with high apparent affinity. Conformational movements of the ATP binding domain were determined using the fluorescent analog 2′(3′)-O-(2,4,6-trinitrophenyl)adenosine 5′-triphosphate. To assess the conformational behavior of the Ca^{2+} binding domain, we also studied the occlusion of Ca^{2+}, both in the presence and in the absence of ATP and with or without vanadate. Results show the existence of occluded species in the presence of vanadate and/or ATP. This allowed the development of a model that describes the transport of Ca^{2+} and its relation with ATP hydrolysis. This is the first approach that uses a conformational study to describe the PMCA P-type ATPase reaction cycle, adding important features to the classical E_1-E_2 model devised using kinetics methodology only.

P-type ATPases are a group of enzymes responsible for active transport of cations across the cell membrane. They use the hydrolysis of ATP as a source of energy and share in common the formation of an acid-stable phosphorylated intermediate as part of their reaction cycle. The plasma membrane calcium pump (PMCA)[4] is a P-type ATPase that participates as an integral part of the Ca^{2+} signaling mechanism from eukaryotic cells (1) and is thus a crucial component of cell function. Detailed structural information about PMCA is currently lacking. Its abundance is ~0.1% of the total protein in the red cell membrane, although it is much more abundant in some specialized cells. Unfortunately, these latter cells are not available in quantity, hampering efforts to produce suitable crystals for x-ray structure analysis. Although PMCA could not yet be crystallized, insight into the structural organization of the sarcoplasmic reticulum Ca^{2+}-ATPase (SERCA), a member of the same family, has come from the elucidation of several crystal structures at atomic resolution, representing the pump in various intermediate states (see Refs. 2 and 3). The membrane-buried region of SERCA is made up of 10 membrane-spanning helices and is connected to a large cytoplasmic headpiece, which is further separated into three distinct domains, denoted A ("actuator"), P ("phosphorylation"), and N ("nucleotide binding"). However, unlike SERCA, PMCA is highly regulated by calmodulin, which activates this protein by binding to an autoinhibitory region (4) and changes the conformation of the pump from an inhibited state, E_1I, to an activated one, E_1A (4–6).

The current kinetic model for the PMCA proposes that the enzyme exists in two main conformations, E_1 and E_2. E_1 has a high affinity for Ca^{2+} and is readily phosphorylated by ATP, whereas E_2 has a low affinity for Ca^{2+} and can be phosphorylated by P_i. After binding of intracellular Ca^{2+} to high affinity sites, E_1 can be phosphorylated by ATP with formation of the intermediate E_1P. A subsequent conformational transition to E_2P would allow Ca^{2+} to be released to the extracellular medium from low affinity sites, followed by the hydrolysis of the phosphoenzyme to E_2 and a new conformational transition to E_1 (7). During some stages of the reaction cycle, Ca^{2+} becomes occluded (*i.e.* trapped in the enzyme machinery) while it is transported from one side to the other side of the membrane (8). It has been described that in addition to being the substrate in the phosphorylation of the E_1Ca state, ATP also functions in a non-phosphorylating mode by enhancing the rates of the

* This work was supported by the Agencia Nacional de Promoción Científica y Tecnológica, Consejo Nacional de Investigaciones Científicas y Técnicas, and Universidad de Buenos Aires Ciencia y Técnica (UBACYT; Argentina).
[1] Both authors contributed equally to this work.
[2] To whom correspondence may be addressed. E-mail: rcr@retina.ar.
[3] To whom correspondence may be addressed. E-mail: jprossi@qb.ffyb.uba.ar.
[4] The abbreviations used are: PMCA, plasma membrane calcium pump; DMPC, 1,2-dimyristoyl-*sn*-glycero-3-phosphocholine; $C_{12}E_{10}$, polyoxyethylene-10-dodecyl ether; [^{125}I]TID-PC/16, 1-*O*-hexadecanoyl-2-*O*-[9-[[[2-[^{125}I]iodo-4-(trifluoromethyl-3H-diazirin-3-yl)benzyl]oxy]carbonyl]nonanoyl]-*sn*-glycero-3-phosphocholine; SERCA, sarcoplasmic reticulum Ca^{2+}-ATPase; Tricine, *N*-[2-hydroxy-1,1-bis(hydroxymethyl)ethyl]glycine; ASA, accessible surface area; TNP-ATP, 2′(3′)-*O*-(2,4,6-trinitrophenyl)adenosine 5′-triphosphate.

steps involved in phosphoenzyme turnover ($E_1PCa \rightarrow E_2P$ and $E_2P \rightarrow E_2$) as well as the $E_2 \rightarrow E_1Ca$ transition of the dephosphoenzyme (9–20). In PMCA, the mechanisms underlying these modulatory effects of ATP remain largely unresolved.

By using [^{125}I]TID-PC/16, we were previously able to assess different transmembrane conformations in PMCA: a first one in which the protein displays maximum lipid exposure corresponding to an autoinhibited state of the enzyme (E_1CaI, in the presence of Ca^{2+} alone, hereafter denoted as E_1Ca), a second one in which protein-lipid interactions are markedly decreased corresponding to an activated state (E_1CaA, presence of Ca^{2+} and calmodulin), and a third one in the absence of Ca^{2+} (E_2) (21). Using the same experimental approach, we were also able to measure equilibrium constants for different ligands through the change of transmembrane conformations in PMCA (22). In order to obtain a complete understanding of the physical processes that involve ATP hydrolysis and Ca^{2+} transport, it is necessary to know more about the structure of the enzyme. The above results highlight the convenience of directly exploring the effects of different ligands on the PMCA transmembrane region. Applying this technique to PMCA, we were able to measure equilibrium constants for the dissociation of ligands from PMCA complexes and to draw structural conclusions about the regulation of the transport of Ca^{2+} in the presence of different ligands, such as ATP and vanadate, a well known inhibitor of P-ATPases, which forms a complex analogous to the phosphorylated intermediate E_2P. Conformational movement of the ATP binding domain was determined using the fluorescent analog TNP-ATP. To assess the conformational behavior of the Ca^{2+} domain, we also studied the occlusion of Ca^{2+} in experimental conditions that lead the PMCA to different intermediates of the reaction cycle.

EXPERIMENTAL PROCEDURES

Reagents—All chemicals used in this work were of analytical grade and purchased mostly from Sigma. Recently drawn human blood for the isolation of PMCA was obtained from the Hematology Section of Fundacion Fundosol (Argentina). Blood donation in Argentina is voluntary, and therefore the donor provides informed consent for the donation of blood and for the subsequent legitimate use of the blood by the transfusion service. None of the experiments described in this paper included calmodulin in the incubation media, and therefore, all results refer to the autoinhibited form of the PMCA.

Purification of PMCA from Human Erythrocytes—PMCA was isolated from calmodulin-depleted erythrocyte membranes by the calmodulin affinity chromatography procedure (23). Protein concentration after purification was about 10 μg/ml. No phospholipids were added at any step along the purification procedure. The purification procedure described preserves transport activity and the kinetic properties and regulatory characteristics of the enzyme in its native milieu (23, 24).

Measurement of Ca^{2+}-ATPase Activity—Ca^{2+}-ATPase activity was measured at 37 °C as the initial velocity of release of P_i from ATP, as described previously (7). The incubation medium contained 40 μM DMPC, 120 μM $C_{12}E_{10}$, 120 mM KCl, 30 mM MOPS-K (pH 7.4 at 37 °C), 2 mM ATP, 3.75 mM $MgCl_2$, 2 mM EGTA, and enough $CaCl_2$ to give 100 μM final free [Ca^{2+}]. When necessary, sodium orthovanadate ($(VO_4)^{3-}$, also named vanadate hereafter) or lanthanum chloride (La^{III}) was added at the concentrations indicated in the figures. Release of P_i was estimated according to the procedure of Fiske and SubbaRow (25). Measurements were performed in a Jasco V-630 Bio spectrophotometer.

Determination of Phosphorylated Intermediates—The phosphorylated intermediates (*E*P) were measured as the amount of acid-stable ^{32}P incorporated into the enzyme (0.9 μg/ml), according to the method described by Echarte *et al.* (26). The phosphorylation was measured at 4 °C in a medium containing 30 mM MOPS-K (pH 7.4 at 4 °C), 120 mM KCl, 3.75 mM $MgCl_2$, 120 μM $C_{12}E_{10}$, 40 μM DMPC, 2 mM EGTA, 30 μM [γ-^{32}P]ATP, and enough $CaCl_2$ to obtain 100 μM final free [Ca^{2+}]. The reaction was started by the addition of [γ-^{32}P]ATP under vigorous stirring, and after 1 min, it was stopped with an ice-cold solution of TCA (10% (w/v) final concentration). The tubes were centrifuged at 7000 rpm for 3.5 min at 4 °C. The samples were then washed once with 7% TCA, 150 mM H_3PO_4 and once with double-distilled water and processed for SDS-PAGE. For this purpose, the pellets were dissolved in a medium containing 150 mM Tris-HCl (pH 6.5 at 14 °C), 5% SDS, 5% DTT, 10% glycerol, and bromphenol blue (sample buffer). Electrophoresis was performed at pH 6.3 (14 °C) in a 7.5% polyacrylamide gel. The reservoir buffer was 0.1 M sodium phosphate, pH 6.3, with 0.1% SDS. Migration of the sample components took place at 14 °C, with a current of 60 mA until the tracking dye reached a distance of about 10 cm from the top of the gel. Gels were stained, dried, and exposed to a Storage Phospho Screen (Amersham Biosciences). Unsaturated autoradiograms and stained gels were scanned with an HP Scanjet G2410 scanner. Analysis of the images was performed with GelPro Analyzer. *E*P quantification was achieved as described by Echarte *et al.* (26).

Preparation of [^{125}I]TID-PC/16—TTD-PC/16 (tin precursor) was a kind gift of Dr. J. Brunner (ETH Zentrum, Zurich, Switzerland). [^{125}I]TID-PC/16 was prepared by radioiodination of its tin precursor according to Weber and Brunner (27).

Labeling—A photolabeling assay was carried out as described by Mangialavori *et al.* (21, 22). A dried film of the photoactivatable reagent was suspended in PC/$C_{12}E_{10}$ mixed micelles containing 10 μg/ml of the membrane protein. The samples were incubated in the presence of necessary components for 10 min at 25 °C before being irradiated for 10 min with light from a filtered UV source (λ = 360 nm).

Radioactivity and Protein Determination—Electrophoresis was performed according to the Tris-Tricine SDS-PAGE method (28). Polypeptides were stained with Coomassie Blue R; the isolated bands were excised from the gel, and the incorporation of radioactivity was directly measured on a γ-counter. The amount of protein was quantified by eluting each stained band, as described previously (29), including bovine serum albumin in each gel as a standard for protein quantification. Specific incorporation was calculated as the ratio between the measured radioactivity and the amount of protein determined for each band. In all cases, a sample in the presence of 2 mM EGTA was included as a control and was taken as 100% of the specific incorporation. This condition was included in the figures only when it was necessary for the result analysis.

Measurements of Occluded Calcium—The procedure for measuring the occlusion of Ca^{2+} in microsomes containing PMCA involves a system for overexpression of the PMCA and the use of a rapid mixing device combined with a filtration chamber, allowing the isolation of the enzyme and quantification of calcium occluded (8, 30). In a typical experiment, one volume of a microsomal preparation suspended in a solution with 30 mM MOPS-K (pH 7.4 at 25 °C), 120 mM KCl, and 400 nM thapsigargin was mixed with the same volume of a solution containing the same concentrations of MOPS-K and KCl plus 3.75 mM $MgCl_2$, 2 mM ATP, and enough $[^{45}Ca^{2+}]CaCl_2$ to obtain the concentrations of free Ca^{2+} indicated in the figures. For some experiments, either 50 μM $(VO_4)^{3-}$ or 50 μM La^{III} (in this case, to minimize the possibility of precipitation with La^{III}, ATP was 25 μM instead of 2 mM) was also included in the latter solution. Measurements were carried out in equilibrium conditions at 25 °C. To ensure the achievement of equilibrium, a reaction time of 3 s was selected after measuring the time courses of occluded calcium in different incubation media. Reactions were quenched by injecting the reaction mixture into the filtration chamber (quenching and washing chamber) at a flow rate of 1–5 ml/s. During the injection process, the fluid was mixed with an ice-cold washing solution flowing at a rate of 30–40 ml/s and then filtered through a Millipore filter (AA, 0.8-μm pore size) placed in the quenching and washing chamber in order to retain the microsomal suspension that included the enzyme. To ensure that the initial temperature in the quenching and washing chamber was 1–2 °C and that the flow was constant, about 50 ml of washing solution was allowed to run through the filter prior to the injection of the reaction mixture, and 240 ml of washing solution was applied to the filter thereafter. The composition of the washing solution was 10 mM Tris (pH 7.4 at 2 °C) and 10 mM EDTA. After the washing solution was drained, the filter was removed, dried under a lamp, and counted for $^{45}Ca^{2+}$ radioactivity in a scintillation counter. This was converted into nmol of Ca^{2+} using the specific activity value of the $^{45}Ca^{2+}$ in the reaction mixture. Ca^{2+} occluded was considered equal to the $^{45}Ca^{2+}$ radioactivity retained by the enzyme after subtracting the blank values. These were estimated from the amount of $^{45}Ca^{2+}$ retained by the filters in the presence of enzyme that was heat-inactivated for 2 h at 50 °C.

Spectroscopic Measurements—The fluorescence measurements were made in a quartz cell of 3 × 3 mm using an SLM-spectrofluorometer AMINCO BOWMAN Series 2 (Spectronic Instrument Inc., Rochester, NY). The excitation and emission bandwidths were set at 4 nm.

Determination of PMCA Apparent Affinity for TNP-ATP—Purified PMCA (10 μg/ml) was reconstituted in a medium containing 40 μM DMPC, 120 μM $C_{12}E_{10}$, 120 mM KCl, 30 mM MOPS-K (pH 7.4 at 25 °C), 1 mM $MgCl_2$ and then incubated with one of the following components for 10 min at 25 °C: (i) 2 mM EGTA, (ii) 100 μM free Ca^{2+}, (iii) 2 mM EGTA plus 50 μM $(VO_4)^{3-}$, or (iv) 100 μM free Ca^{2+} plus 50 μM $(VO_4)^{3-}$. After incubation, increasing concentrations of TNP-ATP were added to each condition as described previously by Qu *et al.* (31). The fluorescence emission was measured at 539 nm after excitation at 495 nm and corrected for light scattering by background subtraction. An aliquot of the same solution without protein was titrated as a control in all experiments. In this case, the fluorescence emission behavior of TNP-ATP was linear and less than 15% of the fluorescence emission in the presence of protein.

As described previously by Pérez-Gordones *et al.* (32), in the presence of calcium, no hydrolysis was observed of TNP-ATP. As was reported for other ATPases (33–37), PMCA Ca^{2+}-ATPase activity is completely inhibited by this analog.

Analysis of SERCA Structure and Accessible Surface Area (ASA)—The ASAs of two crystal structures of SERCA were compared as an approach to analyze the changes in incorporation of $[^{125}I]$TID-PC/16 in the PMCA intermediates E_1Ca and E_1PCa. The crystal structures used for comparison were those of $E_1{\cdot}2Ca$ (Protein Data Bank code 1su4) (38) and Ca_2E_1P (Protein Data Bank code 3ba6) (39). The transmembrane regions were taken as explicitly defined in Uniprot for sarcoplasmic/endoplasmic reticulum calcium ATPase 2, accession number P20647. The ASA of the transmembrane helices was calculated with MolMol (40, 41) with a solvent radius of 1.4 Å.

Data Analysis—Theoretical equations were fitted to the results by nonlinear regression based on the Gauss-Newton algorithm using commercial programs (Excel and Sigma-Plot for Windows, the latter providing not only the best fitting values of the parameters but also their S.E.). The goodness of fit of a given equation to the experimental results was evaluated by the corrected AIC criterion (42) defined as $AIC_C = N \ln(SS/N) + 2PN/(N - P - 1)$, where N is the number of data, P is the number of parameters plus one, and SS is the sum of weighted square residual errors. Unitary weights were considered in all cases, and the best equation was chosen as that giving the lower value of AIC_C. The AIC criterion is based on information theory and selects an equation among several possible equations on the basis of its capacity to explain the results using a minimal number of parameters.

RESULTS

Effect of Vanadate and Lanthanum on PMCA Ca^{2+}-ATPase Activity—Ca^{2+}-ATPase activity of purified PMCA was measured in the presence of 100 μM free Ca^{2+} and increasing concentrations of vanadate (Fig. 1*A*) or La^{III} (Fig. 1*B*). Equation 1 was fitted to the experimental data (continuous lines),

$$v = \frac{V_0 K_I}{K_I + [I]} \qquad \text{(Eq. 1)}$$

where $[I]$ is the concentration of inhibitor (either $(VO_4)^{3-}$ or La^{III}), V_0 is the Ca^{2+}-ATPase activity in the absence of inhibitor, and K_I is the concentration of inhibitor needed for half-maximal effect. The value of K_I for $(VO_4)^{3-}$ was 1.5 ± 0.1 μM, and it was similar to that reported previously (43), and the value of K_I found for La^{III} was 8.2 ± 0.5 μM.

Although these inhibitors have similar effects on the PMCA activity, vanadate mimics the phosphoryl group in the transition state of E_2P, preventing the enzyme phosphorylation (Fig. 1*A*, *inset*) (43–45), whereas La^{III} inhibits by blocking the transition $E_1P \rightarrow E_2P$, acting noncompetitively with respect to Ca^{2+} and ATP and bringing the enzyme phosphorylation level to a maximum (Fig. 1*B*, *inset*) (46, 47).

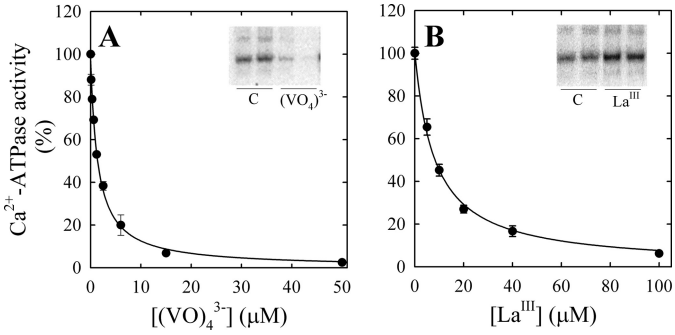

FIGURE 1. **Effect of vanadate (*A*) and lanthanum (*B*) on PMCA Ca^{2+}-ATPase activity.** PMCA Ca^{2+}-ATPase activity was determined as described under "Experimental Procedures" and normalized according to the activity obtained in the absence of $(VO_4)^{3-}$ or La^{III}. The *continuous line* represents the fit of Equation 1 to the experimental values. The apparent K_i for the complexes of PMCA with $(VO_4)^{3-}$ and La^{III} were 1.5 ± 0.1 and 8.2 ± 0.5 μM, respectively. *Insets*, gel autoradiographs of the phosphorylated intermediates of PMCA obtained in the absence of vanadate (control (*C*)) or in the presence of 50 μM $(VO_4)^{3-}$ (*A*) or 100 μM La^{III} (*B*).

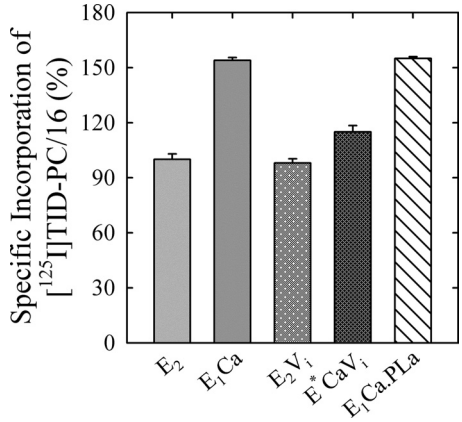

FIGURE 2. **Effect of different ligands on the conformation of PMCA.** Specific incorporation of [^{125}I]TID-PC/16 into PMCA was determined as described under "Experimental Procedures" in the presence of 2 mM EGTA (E_2); 100 μM free Ca^{2+} (E_1Ca); 50 μM $(VO_4)^{3-}$ plus 2 mM EGTA (E_2V_i); 50 μM $(VO_4)^{3-}$ plus 100 μM free Ca^{2+} (E^*CaV_i); or 50 μM La^{III}, 100 μM free Ca^{2+} plus 25 μM ATP ($E_1PCa{\cdot}La$). Specific incorporation of the probe in the presence of 2 mM EGTA (E_2) was taken as 100%. *Error bars*, S.E.

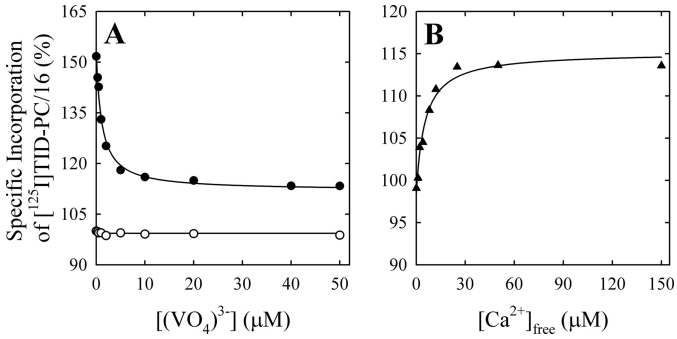

FIGURE 3. **Effect of vanadate on the conformation of the transmembrane domain of PMCA.** *A*, specific incorporation of [^{125}I]TID-PC/16 to PMCA in the presence of 2 mM EGTA (*open circles*) or 100 μM free Ca^{2+} (*closed circles*) at increasing $(VO_4)^{3-}$ concentrations. The *continuous line* in the presence of calcium is the graph of Equation 2 using the best fitting parameters in Table 1 (Reaction ii). Specific incorporation of [^{125}I]TID-PC/16 to PMCA in the presence of 2 mM EGTA as a function of $[(VO_4)^{3-}]$ was constant (*continuous line*; Reaction vi), and thus K_x could not be experimentally determined. *B*, specific incorporation of [^{125}I]TID-PC/16 to PMCA in the presence of 50 μM $(VO_4)^{3-}$ and increasing free Ca^{2+} concentrations. The *continuous line* is the graph of Equation 3 using the best fitting parameters shown in Table 1 (Reaction iii). Specific incorporation of the probe in the presence of 2 mM EGTA was taken as 100%.

Effects of Vanadate and Lanthanum on the PMCA Transmembrane Domain Conformation—To investigate the structure-function relationship of intermediates of the reaction cycle of PMCA, we studied the effects of $(VO_4)^{3-}$ and La^{III} on the conformation of the transmembrane domain of the pump under conditions similar to those used in the inhibition experiments of Fig. 1, except for the fact that all experiments were performed in equilibrium. To this end, we used a hydrophobic photolabeling strategy with [^{125}I]TID-PC/16, a photoactivatable reagent that has been previously shown to behave as phosphatidylcholine with regard to protein-lipid interactions (48, 49). It is thus possible to assess lipid exposure of transmembrane protein regions by quantifying the amount of reagent that becomes covalently attached to the protein upon photolysis (6, 21, 22, 48–52). In order to ensure equilibrium conditions, ATP was omitted from the media except when La^{III} was present.

First, we determined the extent of [^{125}I]TID-PC/16 labeling of the PMCA in its major known conformational states. The E_1Ca conformer is obtained by incubating the enzyme in the presence of Ca^{2+} alone, whereas in the presence of 2 mM EGTA, the conformational equilibrium is shifted toward the E_2 state (in the absence of Ca^{2+}), whose level of [^{125}I]TID-PC/16 incorporation was taken as 100% (21). Because in this work we do not analyze the effect of calmodulin, we simply refer to the state of PMCA plus Ca^{2+} as E_1Ca. In the E_1Ca conformer, the incorporation of [^{125}I]TID-PC/16 increases by 50% as compared with that of E_2. The $E_1PCa{\cdot}La$ conformer was obtained by phosphorylation in the presence of La^{III}, whereas E_2P was mimicked by the complexes of PMCA with $(VO_4)^{3-}$, both with and without Ca^{2+}. Fig. 2 shows the specific incorporation of [^{125}I]TID-PC/16 to PMCA in the presence of EGTA (E_2); Ca^{2+} (E_1Ca); $(VO_4)^{3-}$ plus EGTA (E_2V_i); $(VO_4)^{3-}$ plus Ca^{2+} (E^*V_iCa); or La^{III}, Ca^{2+}, and ATP ($E_1PCa{\cdot}La$). In agreement with reported data (21) specific incorporation of [^{125}I]TID-PC/16 to PMCA was about 55% higher in the E_1Ca conformation than in E_2. In the presence of EGTA, vanadate has no significant effect on the specific incorporation of [^{125}I]TID-PC/16 (98 ± 2.3%). However, whenever Ca^{2+} was present together with vanadate, the area accessible to lipids was different from that obtained in the presence of vanadate or Ca^{2+} alone (115 ± 3.4%). On the other hand, the specific incorporation of [^{125}I]TID-PC/16 in the presence of Ca^{2+}, La^{III}, and ATP was 155.0 ± 1.0%, a value similar to that obtained in the presence of Ca^{2+} alone.

Earlier experiments on the kinetics of vanadate inhibition (53) showed antagonism by Ca^{2+}, consistent with Ca^{2+} and $(VO_4)^{3-}$ binding to alternate conformations. Results obtained with vanadate plus calcium might be explained by two possible hypotheses: (i) the state denoted as E^*V_iCa is actually an equilibrium mixture of mutually exclusive states of PMCA, E_2V_i, and E_1Ca, or (ii) both Ca^{2+} and $(VO_4)^{3-}$ can bind together to PMCA in a state, E^*V_iCa, where the asterisk indicates a distinct conformation with characteristics of both E_1 and E_2.

In order to test these hypotheses, we measured the specific incorporation of [^{125}I]TID-PC/16 as a function of vanadate concentration (Fig. 3*A*) in media with (*closed circles*) and without (*open circles*) Ca^{2+}. It can be seen that in the latter case,

TABLE 1

Parameters for the interaction of PMCA with calcium, vanadate, and ATP determined from the specific incorporation of [^{125}I]TID-PC/16 under equilibrium conditions (Equations 2 and 3)

E represents the enzyme in the absence of calcium and is supposed to be an equilibrium mixture of the conformational states E_1 and E_2 ([E] = [E_1] + [E_2]), which is shifted toward E_2. E* represents a state formed in the presence of vanadate and calcium whose conformation is different from that of E_1 and E_2. The parameters PC_0 and PC_∞ are the specific incorporation of [^{125}I]TID-PC/16 in the absence of reactants or when their concentration tends to infinity, respectively. K_x is the apparent dissociation constant of the complex of PMCA formed through the corresponding equilibrium reaction on the left. Data for reaction (i), which were included for comparison, were taken from Ref. 22.

	Reaction	Specific incorporation of [^{125}I]TID-PC/16 (%)		Apparent dissociation constant (μM)
		PC_0	PC_∞	K_x
(i)	$E + Ca^{2+} \leftrightarrow E_1Ca$	100.2 ± 0.7	152.2 ± 2.0	0.5 ± 0.1
(ii)	$E_1Ca + (VO_4)^{3-} \leftrightarrow E^*ViCa$	152.9 ± 2.1	112.0 ± 0.8	1.1 ± 0.1
(iii)	$E_2V_i + Ca^{2+} \leftrightarrow E^*V_iCa$	98.5 ± 0.9	114.1 ± 2.2	5.3 ± 1.3
(iv)	$E + ATP \leftrightarrow EATP$	100.3 ± 1.8	82.7 ± 0.7	19.9 ± 4.0
(v)	$E_2V_i + ATP \leftrightarrow E_2V_iATP$	99.9 ± 0.9	85.3 ± 0.6	7.6 ± 1.1
(vi)	$E + (VO_4)^{3-} \leftrightarrow E_2V_i$	99.3 ± 0.5	99.3 ± 0.5	-
(vii)	$EATP + (VO_4)^{3-} \leftrightarrow E_2V_iATP$	86.3 ± 0.4	86.3 ± 0.4	-
(viii)	$E^*V_iCa + ATP \leftrightarrow E^*V_iCaATP$	112.6 ± 2.9	91.2 ± 1.2	9.0 ± 2.7
(ix)	$E_1Ca + La^{III} + 2\ ATP \leftrightarrow E_1CaP{\cdot}LaATP + ADP$	154.4 ± 2.6	154.4 ± 2.6	-

specific incorporation is independent of [$(VO_4)^{3-}$], indicating that the E_2 and the E_2P analog conformations have similar areas accessible to lipids. The average value of the specific incorporation is around 100% (99.3 ± 0.5%; Table 1). In the presence of Ca^{2+}, however, there is a decrease of specific incorporation that tends to a level significantly higher than 100%. Results in Fig. 3*A* (*closed circles*) were analyzed by nonlinear fitting of the following decreasing function of [$(VO_4)^{3-}$],

$$PC = PC_\infty + \frac{(PC_0 - PC_\infty)\,K_X}{K_X + [X]} \qquad \text{(Eq. 2)}$$

where PC is the specific incorporation of [^{125}I]TID-PC/16; [X] is the concentration of vanadate; PC_0 and PC_∞ are specific incorporations in the absence of vanadate and at nonlimiting concentration of the inhibitor, respectively; and K_X is the concentration of vanadate for half-maximal effect. This analysis shows (Table 1) that the value of PC_∞ is significantly higher than 100%, making hypothesis (i) above untenable because if E_2V_i and E_1Ca were two mutually exclusive species in equilibrium, the addition of enough vanadate should bring the entire enzyme to the E_2V_i state. We therefore conclude that there exists a ternary complex, E^*V_iCa, which is confirmed by results of titration by Ca^{2+} of E_2V_i (Fig. 3*B*). To analyze these results, Equation 2 above was rearranged to the following increasing hyperbolic function of [Ca^{2+}],

$$PC = PC_0 + \frac{(PC_\infty - PC_0)[X]}{K_X + [X]} \qquad \text{(Eq. 3)}$$

where [X] is now the concentration of Ca^{2+}, PC_0 and PC_∞ are specific incorporations of [^{125}I]TID-PC/16 in the absence of

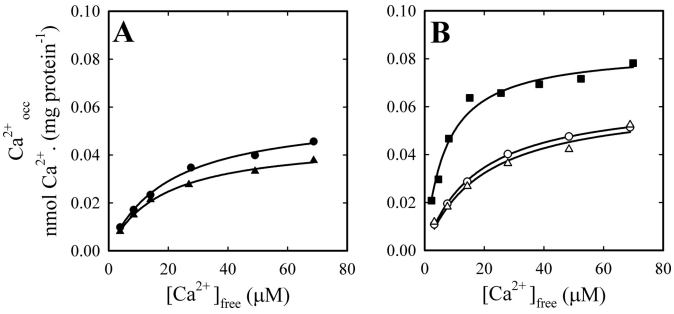

FIGURE 4. **Effect of vanadate on the level of calcium occluded by the PMCA.** Occluded calcium was determined for increasing Ca^{2+} concentrations, with (*triangles*) or without (*circles* and *squares*) 50 μM $(VO_4)^{3-}$ (see "Experimental Procedures" for details). Determinations where performed in the absence (*A*) and in the presence (*B*) of 2 mM ATP, except for a control experiment (*closed squares*), where media contained 25 μM ATP and 50 μM La^{III}. The *continuous lines* represent the fit of a Michaelis-Menten-like function of [Ca^{2+}] to the experimental data. Best fitting values of the parameters were as follows. *A*, *closed circles*, $Ca_{occ,max}$ = 0.058 ± 0.002 nmol of ^{45}Ca (mg of protein)$^{-1}$, $K_{0.5}$ = 19.7 ± 1.9 μM; *closed triangles*, $Ca_{occ,max}$ = 0.046 ± 0.001 nmol of ^{45}Ca (mg of protein)$^{-1}$, $K_{0.5}$ = 17.4 ± 1.4 μM. *B*, *open circles*, $Ca_{occ,max}$ = 0.064 ± 0.001 nmol of ^{45}Ca (mg of protein)$^{-1}$, $K_{0.5}$ = 17.2 ± 0.7 μM; *open triangles*, $Ca_{occ,max}$ = 0.063 ± 0.005 nmol of ^{45}Ca (mg of protein)$^{-1}$, $K_{0.5}$ = 19.1 ± 4 μM; *closed squares*, $Ca_{occ,max}$ = 0.084 ± 0.003 nmol of ^{45}Ca (mg of protein)$^{-1}$, $K_{0.5}$ = 6.8 ± 0.9 μM.

Ca^{2+} and at [Ca^{2+}] tending to infinity, respectively, and K_X is the concentration of Ca^{2+} for half-maximal effect. In this case, the value of PC_∞ is 114.1 ± 2.2%, which is not significantly different from the value of 112 ± 0.8% obtained from the titration of E_1Ca with vanadate. These values indicate that the addition of enough Ca^{2+} to the enzyme-vanadate complex (Fig. 3*B*) and the addition of enough vanadate to the E_1Ca complex (Fig. 3*A*, *closed circles*) lead to the same ternary complex, E^*V_iCa.

These results suggest that, despite the apparent lack of effect of vanadate in Fig. 3*A* (*open circles*), the addition of Ca^{2+} reveals that E_2 and E_2V_i are different conformers of the pump. From the results in Fig. 3, we postulate the existence of two phosphoenzyme analogs with vanadate: E_2V_i in the absence of calcium and E^*V_iCa in its presence.

Effect of Vanadate on Occluded Intermediates of PMCA—We have previously identified and characterized the calcium occluded intermediate(s) of PMCA using a rapid mixing device combined with a filtration chamber, allowing the isolation of the enzyme and the quantification of occluded calcium (8).

To confirm the existence of the E^*V_iCa intermediate in equilibrium and steady-state conditions, with or without ATP, we measured the amount of occluded calcium in the absence and in the presence of vanadate for different concentrations of Ca^{2+}, in media either without (Fig. 4*A*) or with 2 mM ATP (Fig. 4*B*). We also included a control experiment performed in the absence of vanadate and in the presence of 25 μM ATP plus 50 μM La^{III}. As expected, experimental data for each condition can be described by a rectangular hyperbola as a function of [Ca^{2+}]. In the absence of ATP, vanadate slightly reduces (around 20%) the amount of intermediate with calcium occluded (Fig. 4*A*), whereas the inhibitor has no significant effect in the presence of ATP (Fig. 4*B*). In accordance with the increase of phosphorylated intermediate shown in Fig. 1*B*, the maximal level of occluded intermediate obtained in the presence of La^{III} and ATP is about 30% higher than in the absence of the inhibitor. The addition of lanthanum also increased more than 2.5-fold the apparent affinity for Ca^{2+}.

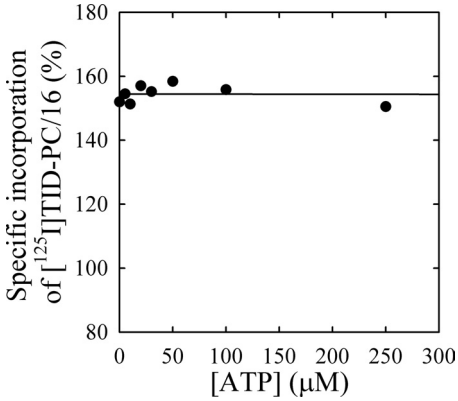

FIGURE 5. **Effect of ATP on the conformation of the transmembrane domain of the E_1PCa analog.** Specific incorporation of [^{125}I]TID-PC/16 to PMCA was determined as a function of increasing ATP concentrations in the presence of 100 μM free Ca^{2+} plus 50 μM La^{III}. Specific incorporation of the probe into PMCA in the presence of 2 mM EGTA was taken as 100%. Results were approximately constant (*continuous line*, but see "Discussion"), and a precise value of K_x could not be determined (see Table 1, Reaction ix).

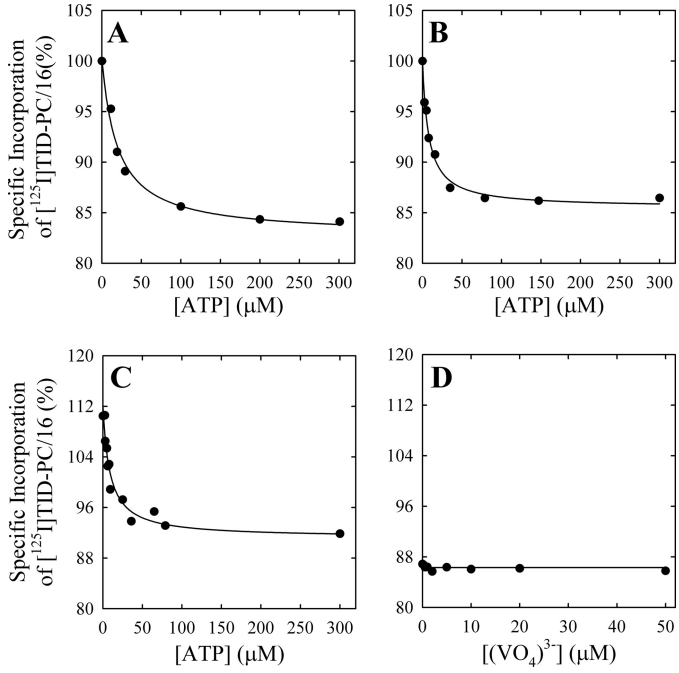

FIGURE 6. **Effect of ATP on the conformation of the PMCA transmembrane domain.** Specific incorporation of [^{125}I]TID-PC/16 to PMCA was determined as a function of increasing ATP concentrations in the presence of 2 mM EGTA (*A*), 2 mM EGTA plus 50 μM $(VO_4)^{3-}$ (*B*), or 100 μM free Ca^{2+} plus 50 μM $(VO_4)^{3-}$ (*C*). The *continuous lines* are the graphs of Equation 2 for the best fitting parameter values shown in Table 1 (Reactions iv, v, and viii, respectively). *D*, the specific incorporation of [^{125}I]TID-PC/16 to PMCA in media with 2 mM EGTA and 2 mM ATP did not vary with the concentration of $(VO_4)^{3-}$ (*continuous line*), and thus K_x could not be experimentally determined (see Table 1, Reaction vii).

The apparent affinity for Ca^{2+} obtained from these experiments was lower than that observed for the purified enzyme, and the effect of vanadate on this was only marginal. Despite the difficulty of comparing data coming from very different preparations (see "Experimental Procedures"), these results confirm that calcium is occluded not only in E_1Ca but also in the E^*V_iCa ternary complex. The higher level of calcium occlusion obtained in the presence of ATP (Fig. 4*B*) would indicate that the nucleotide is able to bind to E^*V_iCa to form a quaternary complex, E^*V_iCaATP.

Effects of ATP—In addition to its role as substrate in the phosphorylation of the E_1 state, ATP also operates in a non-phosphorylating mode (modulatory ATP), enhancing the rates of the steps involved in phosphoenzyme turnover ($E_1P \rightarrow E_2P$ and $E_2P \rightarrow E_2$) as well as the $E_2 \rightarrow E_1$ transition of the dephosphoenzyme (7, 54, 55) The mechanisms underlying these modulatory effects of ATP have been extensively studied in SERCA (9–20). However, for PMCA, this question remains unsolved. Therefore, we employed a strategy similar to that described above to study the transmembrane conformational changes associated with the binding of ATP to different states of PMCA.

E_1PCa State—In order to study the effect of ATP on the conformation of the transmembrane domain during formation of E_1PCa, we measured the specific incorporation of [^{125}I]TID-PC/16 into PMCA as a function of [ATP] in the presence of La^{III} and Ca^{2+} (Fig. 5). In the initial condition, PMCA is in the E_1Ca conformation (46, 47), and as ATP concentration increases, the reaction is shifted toward the formation of the phosphorylated intermediate, $E_1PCa{\cdot}La$ (see Fig. 1*B*, *inset*). Although ATP can also bind to this intermediate with low affinity (55), only marginal effects in specific incorporation of [^{125}I]TID-PC/16 are detected. There appears to be a slight increase at low concentrations of ATP followed by a low affinity decrease at concentrations higher than 50 μM. However, these changes are difficult to ascertain, and it seems safer to describe the phenomenon by saying that the level of [^{125}I]TID-PC/16 incorporation remains approximately constant around the value obtained for E_1Ca (155 ± 1%).

E_2 and E_2P Analog States—On the contrary, titration of the E_2 state with ATP in the absence of Ca^{2+} (Fig. 6*A*) leads to a decrease in specific incorporation of [^{125}I]TID-PC/16. Results were analyzed by nonlinear fitting of Equation 2, where the variable *X* stands for ATP. The best fitting values of the parameters are shown in Table 1. These results show that ATP can bind to PMCA, at micromolar concentrations, in the absence of Ca^{2+}, causing a conformational change in the transmembrane domain.

Fig. 6, *B* and *C*, shows the specific incorporation of [^{125}I]TID-PC/16 to PMCA as a function of [ATP] when the enzyme was preincubated in the presence of vanadate with and without Ca^{2+}, respectively. Nonlinear fitting of Equation 2 (Table 1) yields values of K_X for ATP that are at least 50% lower than that obtained in the absence of vanadate. In addition, the simultaneous presence of vanadate and Ca^{2+} causes the levels of specific incorporation at both zero and non-limiting [ATP] to be higher than the corresponding levels obtained in the absence of Ca^{2+}.

When the pump was incubated in the absence of Ca^{2+} and in the presence of saturating [ATP], the specific incorporation of [^{125}I]TID-PC/16 to PMCA was around 85% (Fig. 6, *A* and *D*). The addition of increasing vanadate concentrations has no effect on the incorporation of the probe (Fig. 6*D*). This result shows that in the absence of calcium, vanadate does not produce changes in the area accessible to the lipid environment of PMCA transmembrane domain, regardless of the conformation reached by the pump in the presence of ATP. As will be

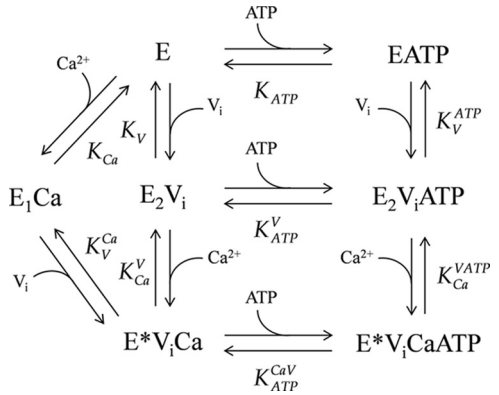

FIGURE 7. **Scheme of the model proposed for the interaction of PMCA with calcium, vanadate, and ATP.** The model was used to perform a global fitting analysis of the results shown in Figs. 3, 5, and 6, and the best fitting values of the parameters are shown in Table 2.

shown below, this lack of effect does not imply the absence of binding of vanadate to PMCA.

A Model for the Interaction of PMCA with Calcium, Vanadate, and ATP—Our findings can be summarized by the scheme shown in Fig. 7. In the absence of Ca^{2+}, PMCA is an equilibrium mixture of 10% E_1 and 90% E_2 forms (56). However, because our experiments do not include information on this equilibrium, we refer to the enzyme in the presence of EGTA as "E", which is an equilibrium mixture of the E_2 and E_1 forms. A similar practice is used for the equilibrium between E_1ATP and E_2ATP, which will depend on the apparent affinities of these forms for the nucleotide, and thus in the absence of calcium, these will simply be denoted as "EATP." On the other hand, our results show that, regarding the conformation of the transmembrane domain, the ternary complex E^*V_iCa is different from E_1Ca and E_2V_i and is therefore denoted with an asterisk, as described above.

Each step in the model represents the equilibrium binding of a single ligand to PMCA. A global fitting of the parameters of the equilibrium equations arising from the model was performed on the results shown in Figs. 3, 5, and 6. The best fitting values for the specific incorporation of [^{125}I]TID-PC/16 (percentage) in the presence of the different reactants and their apparent dissociation constants are shown in Table 2. The parameter values obtained from this global fitting correlate very well with those obtained from each experiment (Table 1), which were taken as initial values for the fitting. The correlation is indicative that this global model is appropriate to describe the interactions of PMCA with Ca^{2+}, vanadate, and ATP. The model allows the determination of the apparent dissociation constants for steps 6, 7, and 8 (*i.e.* for the binding of Ca^{2+} to E_2V_iATP, for the binding of vanadate to E, and for the binding of vanadate to EATP, where the latter two could not be experimentally measured). Results summarized in Table 2 show that (i) the apparent affinity of PMCA for vanadate decreases in the presence of Ca^{2+}, (ii) the apparent affinity of PMCA for Ca^{2+} decreases in the presence of vanadate, (iii) ATP does not modify the apparent affinity for Ca^{2+} of the E_2V_i form, and (iv) the apparent affinity of E_2V_i and E^*V_iCa forms for ATP were similar, meaning that Ca^{2+} does not modify the apparent affinity for ATP of E_2V_i.

TABLE 2

Best fitting values of specific incorporation of [^{125}I]TID-PC/16 and dissociation constants for calcium, vanadate, and ATP predicted by the global model shown in Fig. 7

Constants K_V, K_t^{ATP} and K_{Ca}^{VATP} were calculated as a combination of the rest of the equilibrium constants forming part of the same closed reaction cycle according to the equations, $K_V = K_V^{Ca}K_{Ca}/K_{Ca}^V$, $K_V^{ATP} = K_{ATP}^V K_V/K_{ATP}$, and $K_{Ca}^{VATP} = K_{ATP}^{CaV}K_{Ca}^V/K_{ATP}^V$.

Enzyme species	Specific incorporation of [^{125}I]TID-PC/16 (%)
E_1Ca	153.6 ± 1.2
EATP	85.6 ± 0.9
E_2V_iATP	85.6 ± 0.9
E^*V_iCaATP	91.74 ± 1.1
E^*V_iCa	113.0 ± 0.8
E	99.8 ± 0.8
E_2V_i	99.8 ± 0.8
Dissociation constant	(μM)
K_{Ca}	0.63 ± 0.06
K_V^{Ca}	1.12 ± 0.13
K_{Ca}^V	5.51 ± 1.56
K_{ATP}	12.66 ± 4.53
K_{ATP}^V	7.93 ± 1.80
K_{Ca}^{VATP}	5.05 ± 1.97
K_V	0.13 ± 0.04
K_V^{ATP}	0.08 ± 0.04
K_{ATP}^{CaV}	7.43 ± 1.43

Interaction of TNP-ATP with Different PMCA Intermediates—The previous strategy does not allow for obtaining information about the relationship between ATP and PMCA in the presence of Ca^{2+}, the catalytic role of ATP, because this nucleotide is rapidly hydrolyzed. Therefore, in order to obtain more information on the interaction of E_1Ca or E_2 with ATP, we studied the binding of its non-hydrolyzable, fluorescent analog, TNP-ATP, to PMCA in different conditions. This approach was used for studying the interaction with ATP in several proteins (reviewed in Ref. 57). As was previously reported for PMCA (32) and other proteins (57), TNP-ATP is not a substrate for the pump and inhibits its ATPase activity. Fig. 8 shows the fluorescence at 539 nm as a function of [TNP-ATP] in media where PMCA was incubated with and without 100 μM Ca^{2+} and without (*A*) or with (*B*) 50 μM vanadate. Experimental data can be described by the equation,

$$\Delta F = \frac{\Delta F_{max} \cdot [S]}{K_D + [S]} \qquad \text{(Eq. 4)}$$

which represents the interaction with a single type of binding sites, where ΔF represents the change in fluorescence intensity following the addition of TNP-ATP at a concentration [*S*], ΔF_{max} is the maximum change in fluorescence intensity, and K_D

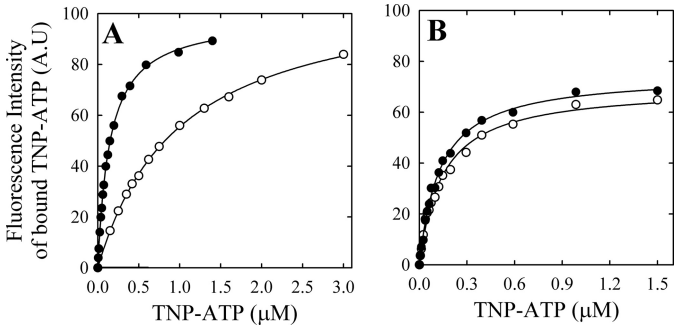

FIGURE 8. **Binding of TNP-ATP to PMCA.** Fluorescence intensity of bound TNP-ATP to PMCA as a function of the concentration of TNP-ATP was determined as described under "Experimental Procedures" in the presence of 100 μM free Ca^{2+} (*closed circles*) or 2 mM EGTA (*open circles*) (*A*) and in the presence of 50 μM $(VO_4)^{3-}$ and either 100 μM free Ca^{2+} (*closed triangles*) or 2 mM EGTA (*open triangles*) (*B*). The *continuous line* is the graph of Equation 4 using the best fitting parameters shown in Table 3.

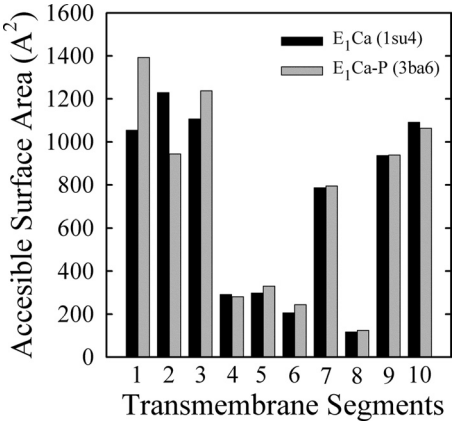

FIGURE 9. **ASAs of the transmembrane domains (helices M1–M10) calculated from the crystal structures 1su4 (E_1Ca_2) and 3ba6 ($E_1P(Ca_2)$) of SERCA.** For details, see "Experimental Procedures."

TABLE 3

PMCA apparent affinity for TNP-ATP under equilibrium conditions

ΔF_{max} corresponds to the fluorescence intensity when the concentration of TNP-ATP tends to infinity, and K_D represents the apparent dissociation constant for the complex formed between PMCA and TNP-ATP. For the meaning of E and E*, see the legend to Table 1.

Reaction	ΔF_{max} (Fluorescence Intensity (A. U))	K_D (μM)
E + TNP-ATP ↔ E*TNP-ATP*	100.2 ± 1.0	1.01 ± 0.07
E_1Ca + TNP-ATP ↔ E_1Ca*TNP-ATP*	99.1 ± 1.2	0.15 ± 0.01
E_2V_i + TNP-ATP ↔ E_2V_i*TNP-ATP*	70.0 ± 1.5	0,13 ± 0.01
E^*V_iCa + TNP-ATP ↔ E^*V_iCa*TNP-ATP*	74.9 ± 1.1	0.15 ± 0.01

is the apparent dissociation constant for the probe. The best fitting values of K_D and ΔF_{max} are shown in Table 3.

Results show that the apparent affinity of PMCA for TNP-ATP is 10-fold higher in the presence of Ca^{2+} than that in its absence. However, in the presence of vanadate, the apparent affinity for this ATP analog did not change with the addition of Ca^{2+} and was similar to that of E_1Ca in Fig. 8*A*. These results can be compared with those in Fig. 6, *A–C*, where the affinity for ATP is clearly higher in the presence of vanadate (*B* and C) than in its absence (*A*), showing a parallel behavior for the affinities of TNP-ATP. It could be surprising that the affinity for ATP observed in Fig. 6 is considerably lower than that for TNP-ATP in Fig. 8. However, Moutin *et al.* (58) reported that the apparent affinity of sarcoplasmic reticulum Ca^{2+}-ATPase for TNP-ATP is significantly higher than that for the unmodified nucleotide.

On the other hand, TNP-ATP fluorescence intensity at saturating concentrations of the probe was similar for E_1Ca and E_2, whereas this value was 40% lower in the presence of vanadate. These results suggest that there is a change in the hydrophobic environment of the TNP-ATP and therefore a different environment for the ATP binding domain as a consequence of the different conformations.

The change in ΔF_{max} upon the addition of vanadate proves that the lack of response to the inhibitor observed in Fig. 3*A* is not due to its inability to bind to PMCA. In other words, vanadate *apparently* does not modify the transmembrane domain, but it does produce a conformational change on the cytoplasmic domain, thus justifying the hypothesis of the existence of a different conformation, E^*V_iCaATP.

DISCUSSION

There are several crystal structures of the Ca^{2+} pump of sarcoplasmic reticulum corresponding to different conformations reached during the reaction cycle (2, 3), and crystal structures of the H^+-ATPase (59) and of the Na^+/K^+-ATPase were reported as well (60, 61). However, there are as yet no high resolution structures for the majority of the P-type ATPases, including the family of PMCAs. This underlines the continued need to develop new tools to probe the structure-function relationship in these proteins by alternative and complementary methods. Of particular interest for a better understanding of the pump mechanism are methods that yield information on the membrane-embedded part of the pump, which is the most difficult region to study by traditional methods of protein expression and analysis.

Effects of Lanthanum and Vanadate on the Transmembrane Domain—For PMCA, the amount of *E*P obtained in the presence of lanthanum is usually considered as a valid calculation of the total active enzyme concentration (55). It has been proposed that La^{III} would act as a dead end inhibitor capable of bringing the entire amount of functionally active enzyme into the E_1PCa form. This phenomenon is consistent with the fact that specific incorporation of [^{125}I]TID-PC/16 in the presence of Ca^{2+}, La^{III}, and ATP was 155.0 ± 1.0%, a maximal value that is similar to that obtained in the absence of ATP. Like the phosphoenzyme level, occlusion of Ca^{2+} is also maximal in the presence of La^{III} and ATP (8). Fig. 5 shows that increasing ATP concentrations produced only marginal changes in the incorporation of [^{125}I]TID-PC/16. This can mean that either (i) significant changes occur in the transmembrane segments, but these are internally counterbalanced, or (ii) La^{III} hinders the transmembrane conformational changes elicited by ATP. As an approach to answer this question, we evaluated the possible extent of this change by calculating the ASA of the transmembrane region using crystallographic data from SERCA. Note that in Protein Data Bank code, the structure of Ca_2E_1P (our E_1PCa) is known as 3ba6, whereas E_1·2Ca (our E_1Ca) is represented by the structure known as 1su4. Results in Fig. 9 show

that most significant changes are found in helices M1–M3, with an increase of 338 Å^2 (32%) for M1, a decrease of 285 Å^2 (30%) for M2, and an increase of 131 Å^2 (12%) for M3. Thus, the overall change in ASA values when the enzyme goes from E_1·2Ca (7113.9 Å^2) to Ca_2E_1P (7349.6 Å^2) is 236 Å^2, just about 3% of the total ASA. These results for SERCA support the idea that our method could be not precise enough to resolve such a small *overall* difference in areas exposed to lipids in PMCA, despite the important changes that can occur in some of the transmembrane segments.

An important conclusion from the above analysis is that, although a difference in the area accessible to lipids can only occur as a consequence of the existence of different conformations of the pump, the opposite is not necessarily true (*i.e.* a similar value of specific incorporation of [^{125}I]TID-PC/16 does not necessarily imply similar conformations), because different arrangements of the transmembrane helices could present a similar surface accessible to lipids.

Vanadate is considered to mimic a pentacoordinated transition state of the phosphoryl group, binding to E_2 in a reaction that requires Mg^{2+} (43, 44). In the absence of Ca^{2+}, vanadate does not produce any detectable change in the specific incorporation of [^{125}I]TID-PC/16 (Fig. 3*A*, *open circles*). However, in the presence of Ca^{2+}, increasing concentrations of vanadate produce a decrease in the specific incorporation of [^{125}I]TID-PC/16 (Fig. 3*A*, *closed circles*). A similar result was obtained when PMCA was incubated with vanadate, and increasing Ca^{2+} concentrations were added (Fig. 3*B*). Inhibition of Ca^{2+}-ATPase activity by vanadate is commonly explained as the result of its binding to the enzyme, leading to a conformation analogous to E_2P. Early experiments on the kinetics of vanadate in SERCA showed that the inhibition is antagonized by Ca^{2+} (44, 53), a result consistent with the idea that Ca^{2+} and vanadate bind to different, mutually exclusive conformations. Experiments by Krebs *et al.* (62) performed in calmodulin-activated PMCA show that vanadate prevents the fluorescence changes that accompany phosphorylation by ATP. However, fluorescence experiments in SERCA (63) suggest the existence of a calcium-enzyme-vanadate complex whose fluorescence properties are "E_1-like" rather than "E_2-like." Our results confirm that in the presence of Ca^{2+} and vanadate, PMCA forms a stable ternary complex, E^*V_iCa, whose conformational state is different from that of E_2 and E_1Ca and that we tentatively designated "E*". Importantly, this ternary complex could be formed in the absence and in the presence of ATP. In agreement with results reported by Daiho *et al.* (64, 65), who obtained a stable transition phosphorylation state of SERCA in the presence of Ca^{2+}, the ternary complex E^*V_iCa could be interpreted as an intermediate state interposed between E_1PCa and the Ca^{2+}-free state E_2P.

While forming the E^*V_iCa complex from E_2V_i, we found that the apparent dissociation constant for Ca^{2+} is higher than in the absence of vanadate (5.1 μM *versus* 1 μM; see Ref. 22). In SERCA (66), biochemical data obtained in the absence of thapsigargin, a potent inhibitor that binds to the transmembrane domain and leads the pump to the E_2 conformation, support the conclusion that the dephosphorylation transition state of E_2P represents a proton-occluded state. This idea arises from the fact that in contrast to E_2, this state has a low affinity for Ca^{2+}. Our results show that a similar state could exist for PMCA.

Ca^{2+} Occlusion—We report here results on Ca^{2+} occlusion obtained in equilibrium conditions, in the absence of ATP or in the presence of ATP plus vanadate. It is a generally accepted idea that in P-type ATPases, occlusion of the cation transported from the cytoplasmic side occurs concomitantly with the formation of E_1P and that the release of the occluded cation toward the opposite side takes place after the E_1P to E_2P conformational transition. This has been proposed both for the occlusion of two calcium ions in the SERCA and of three sodium ions in the Na,K-ATPase. Using membrane-bound PMCA preparations in media with ATP and lanthanum, which blocks the conformational transition from E_1P to E_2P, we found that Ca^{2+} becomes occluded concomitantly with the formation of E_1P with a stoichiometry of one Ca^{2+} per phosphorylated enzyme unit (8). However, this experimental evidence does not exclude the possibility of occlusion of Ca^{2+} in non-phosphorylated intermediates. In this sense, in the absence of ATP, occlusion of Ca^{2+} in SERCA (67) and of Na^+ in oligomycin-inhibited Na,K-ATPase (68) has been reported. This is not surprising if one admits the idea that cation occlusion precedes phosphorylation (or dephosphorylation, depending on the transported cation), thus triggering the reaction (*e.g.* see Refs. 60 and 69).

The increase in affinity for Ca^{2+} observed in the presence of La^{III} can be explained on the basis of the irreversibility of the phosphorylation reaction and the blocking effect of this inhibitor on the E_1P to E_2P conformational transition, which prevents the return of the enzyme to calcium-free states.

Binding of ATP—Toyoshima *et al.* (70) described that in SERCA, the reaction cycle is regulated essentially by Ca^{2+} alone. ATP can bind to the enzyme even when Ca^{2+} is absent, but without Ca^{2+}, the reaction cycle cannot progress. Binding of Ca^{2+} will cause the movement of the transmembrane helices. Fig. 6 shows that ATP binds to PMCA in the absence of Ca^{2+}, and this triggers a change in the transmembrane domain. The apparent dissociation constant for ATP measured with [^{125}I]TID-PC/16 is in agreement with previous reports for SERCA (20). Our results (Fig. 6, *B* and *C*) show that ATP also binds to E_2V_i (an E_2P-like state) and to E^*V_iCa (an E*P(Ca)-like state), producing conformational changes in the PMCA transmembrane domain. Vanadate increases 3-fold the apparent affinity for ATP, both in the presence and in the absence of Ca^{2+}. This is less than the 10-fold increase of the apparent affinity for ATP in SERCA. However, the structural and kinetic analyses of the E_2 conformation of SERCA were performed in the presence of thapsigargin. It was recently suggested (71) that thapsigargin produces stiffness at the transmembrane domain of SERCA, making it unresponsive to conformational changes occurring within the cytosolic domain, and it is unclear how closely these inhibitor-bound structures resemble other, perhaps more physiological, states of the enzyme. In addition, it has been described (72) that in the absence of Ca^{2+}, affinity of SERCA for ATP is lower when thapsigargin is present.

Therefore, those results should not be compared directly with our studies, which were performed in the absence of an inhibitor that leads PMCA to the E_2 conformation. On the con-

trary, our approach measures the actual substrate affinity through the binding of trace amounts of [^{125}I]TID-PC/16, which is directly proportional to the transmembrane surface of PMCA exposed to surrounding lipids.

A most important point of interest is whether binding of nucleotide produces an induced fit prior to the phosphoryl transfer reaction. However, binding of ATP to E_1Ca cannot be measured directly due to the fast setting of a steady state of transport of Ca^{2+} and ATP hydrolysis. We therefore extended our studies of specific conformational effects produced by ATP using its analog TNP-ATP. This fluorescent probe has been used for studying the interaction of several proteins with ATP (53) and is not hydrolyzed by PMCA.

Results shown in Fig. 8 confirm that TNP-ATP binds to PMCA in the absence of Ca^{2+}, although with a higher apparent dissociation constant than that observed in the presence of Ca^{2+} (E_1Ca). At saturating TNP-ATP concentrations, the fluorescence intensity was similar in both conditions, indicating that the hydrophobic environment of the N-domain is also similar, in agreement with results reported in SERCA (2). In PMCA, the apparent K_D values for TNP-ATP of the E_2Vi and E^*V_iCa states were similar to that obtained for the E_1Ca state but 7-fold lower than for E_2.

The maximal fluorescence intensity of the high affinity component for the binding of TNP-ATP was similar for E_2V_i and E^*V_iCa states but significantly lower than that obtained for E_1Ca. This indicates that the N-domain environment is more hydrophobic in the presence of Ca^{2+} (E_1Ca).

A Functional Cycle for PMCA—Scarborough (73) has observed the inadequacy of the E_1/E_2 nomenclature to describe the intermediates involved in the reaction cycle of P-type ATPases. In this work, we have demonstrated the existence of species of PMCA that can be seen as different conformers, depending on whether the measurements were sensing changes in the cytoplasmic (experiments with TNP-ATP) or in the transmembrane ([^{125}I]TID-PC/16 photolabeling) domains of the enzyme. For instance, the apparent lack of effect of vanadate on the transmembrane domain of EATP contrasts with the effect of the inhibitor on the maximal fluorescence change upon binding of TNP-ATP. Although this could mean that significant changes in the transmembrane domain cancel each other regarding their exposure to lipids, as shown above in the case of the structures of $E_1{\cdot}2Ca$ and Ca_2E_1P of SERCA, a possible uncoupling between conformational changes in the cytoplasmic and membrane domains cannot be ruled out and is worth considering. Evidence adding important features to the E_1-E_2 model is that E_2V_i, E_2V_iATP, and E^*V_iCaATP, all of them intermediates that in principle would be thought of as E_2 conformers, actually exhibit different surface areas accessible to phospholipids, which reveals that they should at least be considered as different subconformations.

We have also studied in this work for the first time the effect of ATP on the structure of these subconformations, showing that they are all able to bind ATP at physiological concentrations (see Figs. 6 (*A*–*C*) and 8). This notion questions the physiological relevance of the E_1Ca conformation as an intermediate in the transport scheme, because under physiological conditions, with a concentration of ATP high enough and a large ATP/ADP ratio, the modulatory site will be saturated by ATP, allowing the E_2 state to circumvent the E_1Ca conformation and to transition directly into the E_1ATPCa state.

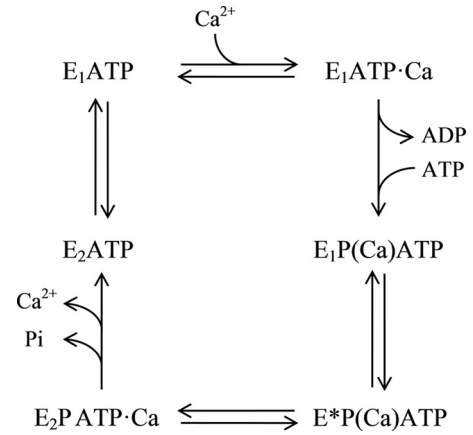

FIGURE 10. **Scheme of the model proposed for the PMCA functional reaction cycle.** *Parentheses* denote cation occlusion.

Taking this evidence together, Fig. 10 shows a functional cycle of ATP binding and hydrolysis by PMCA. Note that (i) we have included a new intermediate, E*P(Ca)ATP, between $E_1P(Ca)ATP$ and $E_2PATP{\cdot}Ca$, whose conformation is different from that of E_1 and E_2, and (ii) with the exception of a transient ADP-bound state, all conformers are bound to a molecule of ATP and can be simultaneously phosphorylated. Conversely, Ca^{2+} can be occluded in or simply bound to the enzyme. In its resting condition, PMCA would mainly exist as two intermediates in equilibrium, E_1ATP and E_2ATP, until a signal of Ca^{2+} or calmodulin-Ca^{2+} initiates the transport of the cation driven by the ATP hydrolysis.

In this study, we focus on the role of ATP in the reaction cycle, leaving aside the effect of cofactors like Mg^{2+} and activators such as calmodulin, which are worthy of future study using the findings of this work as a basis.

Acknowledgments—We are greatly indebted to Dr. Emanuel E. Strehler (Mayo Clinic/Foundation, Rochester, MN) for helpful comments and to Dr. J. Brunner (Swiss Federal Institute of Technology, Zürich) for the kind gift of TTD-PC/16 (tin precursor) and to Fundosol (Argentina).

REFERENCES

1. Strehler, E. E., Caride, A. J., Filoteo, A. G., Xiong, Y., Penniston, J. T., and Enyedi, A. (2007) Plasma membrane Ca^{2+} ATPases as dynamic regulators of cellular calcium handling. *Ann. N.Y. Acad. Sci.* **1099,** 226–236
2. Toyoshima, C. (2009) How Ca^{2+}-ATPase pumps ions across the sarcoplasmic reticulum membrane. *Biochim. Biophys. Acta* **1793,** 941–946
3. Møller, J. V., Olesen, C., Winther, A. M., and Nissen, P. (2010) The sarcoplasmic Ca^{2+}-ATPase. Design of a perfect chemi-osmotic pump. *Q. Rev. Biophys.* **43,** 501–566
4. Sarkadi B., Enyedi, A., Földes-Papp, Z., and Gárdos, G. (1986) Molecular characterization of the *in situ* red cell membrane calcium pump by limited proteolysis. *J. Biol. Chem.* **261,** 9552–9557
5. Corradi, G. R., and Adamo, H. P. (2007) Intramolecular fluorescence resonance energy transfer between fused autofluorescent proteins reveals rearrangements of the N- and C-terminal segments of the plasma membrane Ca^{2+} pump involved in the activation. *J. Biol. Chem.* **282,** 35440–35448

6. Mangialavori, I., Villamil-Giraldo A. M., Pignataro, M. F., Ferreira-Gomes M., Caride A. J., and Rossi J. P. (2011) Plasma membrane calcium pump (PMCA) differential exposure of hydrophobic domains after calmodulin and phosphatidic acid activation. *J. Biol. Chem.* **286,** 18397–18404
7. Rega, A. F., and Garrahan, P. J. (1986) *The Ca^{2+} Pump of Plasma Membranes*, pp. 115–125, CRC Press, Inc., Boca Raton, FL
8. Ferreira-Gomes, M. S., González-Lebrero, R., de la Fuente, M. C., Strehler, E. E., Rossi, R. C., and Rossi, J. P. (2011) Calcium occlusion in plasma membrane Ca^{2+}-ATPase. *J. Biol. Chem.* **286,** 32018–32025
9. Scofano, H. M., Vieyra, A., and de Meis, L. (1979) Substrate regulation of the sarcoplasmic reticulum ATPase. Transient kinetic studies. *J. Biol. Chem.* **254,** 10227–10231
10. Wakabayashi, S., and Shigekawa, M. (1990) Mechanism for activation of the 4-nitrobenzo-2-oxa-1,3-diazole-labeled sarcoplasmic reticulum ATPase by Ca^{2+} and its modulation by nucleotides. *Biochemistry* **29,** 7309–7318
11. McIntosh, D. B., and Boyer, P. D. (1983) Adenosine 5′-triphosphate modulation of catalytic intermediates of calcium ion activated adenosinetriphosphatase of sarcoplasmic reticulum subsequent to enzyme phosphorylation. *Biochemistry* **22,** 2867–2875
12. Wakabayashi, S., Ogurusu, T., and Shigekawa, M. (1986) Factors influencing calcium release from the ADP-sensitive phosphoenzyme intermediate of the sarcoplasmic reticulum ATPase. *J. Biol. Chem.* **261,** 9762–9769
13. Champeil, P., and Guillain, F. (1986) Rapid filtration study of the phosphorylation-dependent dissociation of calcium from transport sites of purified sarcoplasmic reticulum ATPase and ATP modulation of the catalytic cycle. *Biochemistry* **25,** 7623–7633
14. Bodley, A. L., and Jencks, W. P. (1987) Acetyl phosphate as a substrate for the calcium ATPase of sarcoplasmic reticulum. *J. Biol. Chem.* **262,** 13997–14004
15. Shigekawa, M., and Dougherty, J. P. (1978) Reaction mechanism of Ca^{2+}-dependent ATP hydrolysis by skeletal muscle sarcoplasmic reticulum in the absence of added alkali metal salts. II. Kinetic properties of the phosphoenzyme formed at the steady state in high Mg^{2+} and low Ca^{2+} concentrations. *J. Biol. Chem.* **253,** 1451–1457
16. Ariki, M., and Boyer, P. D. (1980) Characterization of medium inorganic phosphate-water exchange catalyzed by sarcoplasmic reticulum vesicles. *Biochemistry* **19,** 2001–2004
17. Champeil, P., Riollet, S., Orlowski, S., Guillain, F., Seebregts, C. J., and McIntosh, D. B. (1988) ATP regulation of sarcoplasmic reticulum Ca^{2+}-ATPase. Metal-free ATP and 8-bromo-ATP bind with high affinity to the catalytic site of phosphorylated ATPase and accelerate dephosphorylation. *J. Biol. Chem.* **263,** 12288–12294
18. Andersen, J. P., and Møller, J. V. (1985) The role of Mg^{2+} and Ca^{2+} in the simultaneous binding of vanadate and ATP at the phosphorylation site of sarcoplasmic reticulum Ca^{2+}-ATPase. *Biochim. Biophys. Acta* **815,** 9–15
19. Clausen, J. D., McIntosh, D. B., Anthonisen, A. N., Woolley, D. G., Vilsen, B., and Andersen, J. P. (2007) ATP-binding modes and functionally important interdomain bonds of sarcoplasmic reticulum Ca^{2+}-ATPase revealed by mutation of glycine 438, glutamate 439, and arginine 678. *J. Biol. Chem.* **282,** 20686–20697
20. Clausen, J. D., McIntosh, D. B., Woolley, D. G., and Andersen, J. P. (2011) Modulatory ATP binding affinity in intermediate states of E_2P dephosphorylation of sarcoplasmic reticulum Ca^{2+}-ATPase. *J. Biol. Chem.* **286,** 11792–11802
21. Mangialavori, I., Villamil Giraldo, A. M., Marino Buslje, C., Ferreira Gomes, M., Caride, A. J., and Rossi, J. P. (2009) A new conformation in sarcoplasmic reticulum calcium pump and plasma membrane Ca^{2+} pumps revealed by a photoactivatable phospholipidic probe. *J. Biol. Chem.* **284,** 4823–4828
22. Mangialavori, I. C., Ferreira-Gomes, M., Pignataro, M. F., Strehler, E. E., and Rossi, J. P. (2010) Determination of the dissociation constants for Ca^{2+} and calmodulin from the plasma membrane Ca^{2+} pump by a lipid probe that senses membrane domain changes. *J. Biol. Chem.* **285,** 123–130
23. Niggli, V., Penniston, J. T., and Carafoli, E. (1979) Purification of the (Ca^{2+}-Mg^{2+})-ATPase from human erythrocyte membranes using a calmodulin affinity column. *J. Biol. Chem.* **254,** 9955–9958
24. Filomatori, C. V., and Rega, A. F. (2003) On the mechanism of activation of the plasma membrane Ca^{2+}-ATPase by ATP and acidic phospholipids. *J. Biol. Chem.* **278,** 22265–22271
25. Fiske, C. H., and SubbaRow, Y. (1925) The colorimetric determination of phosphorus. *J. Biol. Chem.* **66,** 375–400
26. Echarte, M. M., Levi, V., Villamil, A. M., Rossi, R. C., and Rossi, J. P. (2001) Quantitation of plasma membrane calcium pump phosphorylated intermediates by electrophoresis. *Anal. Biochem.* **289,** 267–273
27. Durrer, P., Gaudin, Y., Ruigrok, R. W., Graf, R., and Brunner, J. (1995) Photolabeling identifies a putative fusion domain in the envelope glycoprotein of rabies and vesicular stomatitis viruses. *J. Biol. Chem.* **270,** 17575–17581
28. Schägger, H., and von Jagow, G. (1987) Tricine-sodium dodecyl sulfate-polyacrylamide gel electrophoresis for the separation of proteins in the range from 1 to 100 kDa. *Anal. Biochem.* **166,** 368–379
29. Ball, E. H. (1986) Quantitation of proteins by elution of Coomassie Brilliant Blue R from stained bands after sodium dodecyl sulfate-polyacrylamide gel electrophoresis. *Anal. Biochem.* **155,** 23–27
30. Rossi, R. C., Kaufman, S. B., González-Lebrero, R. M., Nørby, J. G., and Garrahan, P. J. (1999) An attachment for nondestructive, fast quenching of samples in rapid-mixing experiments. *Anal. Biochem.* **270,** 276–285
31. Qu, Q., Russell, P. L., and Sharom, F. J. (2003) Stoichiometry and affinity of nucleotide binding to P-glycoprotein during the catalytic cycle. *Biochemistry* **42,** 1170–1177
32. Pérez-Gordones, M. C., Lugo, M. R., Winkler, M., Cervino, V., and Benaim, G. (2009) Diacylglycerol regulates the plasma membrane calcium pump from human erythrocytes by direct interaction. *Arch. Biochem. Biophys.* **489,** 55–61
33. Lin, S. H., and Faller, L. D. (1996) Estimation of the distance change between cysteine-457 and the nucleotide binding site when sodium pump changes conformation from E1 to E2 by fluorescence energy transfer measurements. *Biochemistry* **35,** 8419–8428
34. Cho, Y. K., Ríos, S. E., Kim, J. J., and Miziorko, H. M. (2001) Estimation of the distance change between cysteine-457 and the nucleotide binding site when sodium pump changes conformation from E_1 to E_2 by fluorescence energy transfer measurements. *J. Biol. Chem.* **276,** 12573–12578
35. Vas, M., Merli, A., and Rossi, G. L. (1994) Antagonistic binding of substrates to 3-phosphoglycerate kinase monitored by the fluorescent analogue 2′(3′)-*O*-(2,4,6-trinitrophenyl)adenosine 5′-triphosphate. *Biochem. J.* **301,** 885–891
36. Huang, S. G., Weisshart, K., and Fanning, E. (1998) Characterization of the nucleotide binding properties of SV40 T antigen using fluorescent 3′(2′)-*O*-(2,4,6-trinitrophenyl)adenine nucleotide analogues. *Biochemistry* **37,** 15336–15344
37. Stewart, R. C., VanBruggen, R., Ellefson, D. D., and Wolfe, A. J. (1998) TNP-ATP and TNP-ADP as probes of the nucleotide binding site of CheA, the histidine protein kinase in the chemotaxis signal transduction pathway of *Escherichia coli*. *Biochemistry* **37,** 12269–12279.
38. Toyoshima, C., Nakasako, M., Nomura, H., and Ogawa, H. (2000) Crystal structure of the calcium pump of sarcoplasmic reticulum at 2.6 Å resolution. *Nature* **405,** 647–655
39. Olesen, C., Picard, M., Winther, A. M., Gyrup, C., Morth, J. P., Oxvig, C., Møller, J. V., and Nissen, P. (2007) The structural basis of calcium transport by the calcium pump. *Nature* **450,** 1036–1042
40. Lee, B., and Richards, F. M. (1971) The interpretation of protein structures. Estimation of static accessibility. *J. Mol. Biol.* **55,** 379–400
41. Koradi, R., Billeter, M., and Wüthrich, K. (1996) MOLMOL. A program for display and analysis of macromolecular structures. *J. Mol. Graph.* **14,** 51–55
42. Burnham, K., P., and Anderson, D., R. (2002) *Model Selection and Multimodel Inference*, 2nd Ed., pp. 60–85, Springer, New York
43. Cantley, L. C., Jr., Cantley, L. G., and Josephson, L. (1978) A characterization of vanadate interactions with the (Na,K)-ATPase. Mechanistic and regulatory implications. *J. Biol. Chem.* **253,** 7361–7368
44. Pick, U. (1982) The interaction of vanadate ions with the Ca-ATPase from sarcoplasmic reticulum. *J. Biol. Chem.* **257,** 6111–6119
45. Rossi, J. P., Garrahan, P. J., and Rega, A. F. (1981) Vanadate inhibition of active Ca^{2+} transport across human red cell membranes. *Biochim. Biophys. Acta* **648,** 145–150

46. Luterbacher, S., and Schatzmann, H. J. (1983) The site of action of La^{3+} in the reaction cycle of the human red cell membrane Ca^{2+}-pump ATPase. *Experientia* **39,** 311–312
47. Herscher, C. J., and Rega, A. F. (1996) Pre-steady-state kinetic study of the mechanism of inhibition of the plasma membrane Ca^{2+}-ATPase by lanthanum. *Biochemistry* **35,** 14917–14922
48. Durrer, P., Galli, C., Hoenke, S., Corti, C., Glück, R., Vorherr, T., and Brunner, J. (1996) H^+-induced membrane insertion of influenza virus hemagglutinin involves the HA2 amino-terminal fusion peptide but not the coiled coil region. *J. Biol. Chem.* **271,** 13417–13421
49. Villamil Giraldo, A. M., Castello, P. R., González-Flecha, F. L., Moeller, J. V., Delfino, J. M., and Rossi, J. P. (2006) Stoichiometry of lipid-protein interaction assessed by hydrophobic photolabeling. *FEBS Lett.* **580,** 607–612
50. Mangialavori, I., Montes, M. R., Rossi, R. C., Fedosova, N. U., and Rossi, J. P. (2011) Dynamic lipid-protein stoichiometry on E_1 and E_2 conformations of the Na^+/K^+-ATPase. *FEBS Lett.* **585,** 1153–1157
51. Mangialavori, I. C., Corradi, G., Rinaldi, D. E., de la Fuente, M. C., Adamo, H. P., and Rossi, J. P. (2012) Autoinhibition mechanism of the plasma membrane calcium pump isoforms 2 and 4 studied through lipid-protein interaction. *Biochem. J.* **443,** 125–131
52. Vanagas, L., de La Fuente, M. C., Dalghi, M., Ferreira-Gomes, M., Rossi, R. C., Strehler, E. E., Mangialavori, I. C., and Rossi, J. P. (2013) Differential effects of G- and F-actin on the plasma membrane calcium pump activity. *Cell Biochem. Biophys.* **66,** 187–198
53. Lytton, J., Westlin, M., Burk, S. E., Shull, G. E., and MacLennan, D. H. (1992) Functional comparisons between isoforms of the sarcoplasmic or endoplasmic reticulum family of calcium pumps. *J. Biol. Chem.* **267,** 14483–14489
54. Reynolds, J. A., Johnson, E. A., and Tanford, C. (1985) Application of the principle of linked functions to ATP-driven ion pumps. Kinetics of activation by ATP. *Proc. Natl. Acad. Sci. U.S.A.* **82,** 3658–3661
55. Echarte, M. M., Rossi, R. C., and Rossi, J. P. (2007) Phosphorylation of the plasma membrane calcium pump at high ATP concentration. On the mechanism of ATP hydrolysis. *Biochemistry* **46,** 1034–1041
56. Adamo H. P., Rega, A. F., and Garrahan, P. J. (1990) The E_2 in equilibrium E_1 transition of the Ca^{2+}-ATPase from plasma membranes studied by phosphorylation. *J. Biol. Chem.* **265,** 3789–3792
57. Hiratsuka, T. (2003) Fluorescent and colored trinitrophenylated analogs of ATP and GTP. *Eur. J. Biochem.* **270,** 3479–3485
58. Moutin, M. J., Cuillel, M., Rapin, C., Miras, R., Anger, M., Lompré, A. M., and Dupont, Y. (1994) Measurements of ATP binding on the large cytoplasmic loop of the sarcoplasmic reticulum Ca^{2+}-ATPase overexpressed in *Escherichia coli*. *J. Biol. Chem.* **269,** 11147–11154
59. Pedersen, B. P., Buch-Pedersen, M. J., Morth, J. P., Palmgren, M. G., and Nissen, P. (2007) Crystal structure of the plasma membrane proton pump. *Nature* **450,** 1111–1114
60. Morth, J. P., Pedersen, B. P., Toustrup-Jensen, M. S., Sørensen, T. L., Petersen, J., Andersen, J. P., Vilsen, B., and Nissen, P. (2007) Crystal structure of the sodium-potassium pump. *Nature* **450,** 1043–1049
61. Shinoda, T., Ogawa, H., Cornelius, F., and Toyoshima, C. (2009) Crystal structure of the sodium-potassium pump at 2.4 Å resolution. *Nature* **459,** 446–450
62. Krebs, J., Vasak, M., Scarpa, A., and Carafoli, E. (1987) Conformational differences between the E_1 and E_2 states of the calcium adenosinetriphosphatase of the erythrocyte plasma membrane as revealed by circular dichroism and fluorescence spectroscopy. *Biochemistry* **26,** 3921–3926.
63. Markus, S., Priel, Z., and Chipman, D. M. (1989) Interaction of calcium and vanadate with fluorescein isothiocyanate labeled Ca^{2+}-ATPase from sarcoplasmic reticulum. Kinetics and equilibria. *Biochemistry* **28,** 793–799
64. Daiho, T., Yamasaki, K., Danko, S., and Suzuki, H. (2007) Critical role of Glu^{40}–Ser^{48} loop linking actuator domain and first transmembrane helix of Ca^{2+}-ATPase in Ca^{2+} deocclusion and release from ADP-insensitive phosphoenzyme. *J. Biol. Chem.* **282,** 34429–34447
65. Daiho, T., Danko, S., Yamasaki, K., and Suzuki, H. (2010) Stable structural analog of Ca^{2+}-ATPase ADP-insensitive phosphoenzyme with occluded Ca^{2+} formed by elongation of A-domain/M1′-linker and beryllium fluoride binding. *J. Biol. Chem.* **285,** 24538–24547
66. Olesen, C., Sørensen T. L., Nielsen, R. C., Møller, J. V., and Nissen P. (2004) Dephosphorylation of calcium pump coupled to counterion occlusion. *Science* **306,** 2251–2255
67. Nakamura, J. (1987) Calcium-dependent calcium occlusion in the sarcoplasmic reticulum Ca^{2+}-ATPase. Its enhancement by phosphorylation of the enzyme. *J. Biol. Chem.* **262,** 14492–14497
68. Esmann, M., Skou, J. C. (1985) Occlusion of Na^+ by the Na,K-ATPase in the presence of oligomycin. *Biochem. Biophys. Res. Commun.* **127,** 857–863
69. Forbush, B., 3rd (1988) Occluded ions and Na,K-ATPase. in *The Na^+,K^+-Pump, Part A*: *Molecular Aspects* (Skou, J. C., Nørby, J. G., Maunsbach, A. B., and Esmann, M., eds) pp. 229–248, Alan R. Liss Inc., New York
70. Toyoshima, C., and Inesi, G. (2004) Structural basis of ion pumping by Ca^{2+}-ATPase of the sarcoplasmic reticulum. *Annu. Rev. Biochem.* **73,** 269–292
71. Akin, B. L., Chen, Z., and Jones, L. R. (2010) Superinhibitory phospholamban mutants compete with Ca^{2+} for binding to SERCA2a by stabilizing a unique nucleotide-dependent conformational state. *J. Biol. Chem.* **285,** 28540–28552
72. Inesi, G., Lewis, D., Ma, H., Prasad, A., and Toyoshima, C. (2006) Concerted conformational effects of Ca^{2+} and ATP are required for activation of sequential reactions in the Ca^{2+} ATPase (SERCA) catalytic cycle. *Biochemistry* **45,** 13769–13778
73. Scarborough, G. A. (2003) Rethinking the P-ATPases problem. *Trends Biochem. Sci.* **28,** 581–594